

Image Sharpness Measurement in Scanning Electron Microscopy—Part II

ANDRÁS E. VLADÁR, MICHAEL T. POSTEK,* MARK P. DAVIDSON†

Hewlett-Packard ULSI Research Laboratory, Palo Alto, California; *National Institute of Standards and Technology, Gaithersburg, Maryland; †Spectel Company, Mountain View, California, USA

Summary: A method for qualitative and quantitative analysis of scanning electron microscope (SEM) images for the determination of sharpness is presented in this paper. Described is a procedure for qualitative analysis based on a software program called SEM Monitor that can be applied to research or industrial SEMs for day-to-day performance monitoring. The idea is based on the fact that, as the electron beam scans the sample, the low-frequency changes in the video signal show information about the larger features and the high-frequency changes give data on finer details. The image contains information about the primary electron beam and about all the parts contributing to the signal formation in the SEM. If everything else is kept unchanged, with a suitable sample, the geometric parameters of the primary electron beam can be mathematically determined. An image of a sample, which has fine details at a given magnification, is sharper if there are more high frequency changes in it. In the SEM, a better focused electron beam yields a sharper image, and this sharpness can be measured. The method described is based on calculations in the frequency domain and can also be used to check and optimize two basic parameters of the primary electron beam, the focus, and the astigmatism.

Key words: scanning electron microscope, electron beam, focus, astigmatism, sharpness, Fourier transform, image analysis, metrology, resolution

Introduction

Any image generated by a scanning electron microscope (SEM) is the result of the sample and electron probe interaction, hence the size and shape of the primary electron beam are among the most important parameters contributing to the quality of that image. The electron beam with a cross section which is smallest in diameter in any direction, that is, closest

in shape to the ideal disk, gives the best achievable resolution. As the primary electron beam is scanned across the sample, electrons, photons, electron-hole pairs, and phonons are generated and a suitable detector converts some of these into a video signal. The low-frequency changes in the video signal contain information about the larger features and the high-frequency changes carry information of finer details. The image also contains information about the primary electron beam and about all the parts contributing to the signal formation in the SEM. When an image is correctly focused, the high-frequency information is maximized, and if this is true for any direction, the astigmatism is minimal.

An image of a sample, which has fine details at a given magnification, is sharper if there are more sample-related high-frequency changes in it. In the SEM, a better focused electron beam yields a sharper image, and this sharpness can be measured. The utility of the sharpness concept for use on production metrology SEMs, as implemented through the Fourier transform technique, has been clearly demonstrated and documented (Postek and Vladár 1998, 1996 a,b). These methods for sharpness analysis, however, were labor intensive and slow and therefore not readily suited for everyday use. Recently, these techniques have been integrated into an easy-to-use, stand-alone hardware and software package called SEM Monitor, which makes the analysis fast and far more convenient and user-friendly. Moreover, this program can serve as a prototype for direct integration into the operational software of an SEM. This paper presents a description of the current system and analytical data taken from both laboratory and semiconductor-integrated circuit production instruments to demonstrate both the relevance of the sharpness concept and the usefulness of this tool for SEM performance monitoring.

Materials and Methods

Scanning Electron Microscopes

The SEMs used in this work were either a digital electronics-equipped Hitachi* S-4000S cold field emission instrument described in the companion paper (Part I, Postek and Vladár 1998) or, for the measurements of semiconductor wafers, a Hitachi S-6280H critical dimension (CD) measurement SEM. The CD expression refers to the size of the smallest feature that a given integrated circuit technology is able to

Contribution of the National Institute of Standards and Technology (NIST). Not subject to copyright.

Address for reprints:

András E. Vladár
Hewlett-Packard ULSI Research Laboratory
3500 Deer Creek Road 25L-3
Palo Alto, CA 94304, USA

fabricate on semiconductor wafers with good productivity. Currently 0.13–0.18 μm CD technologies are under development, while 0.25 μm technologies are already in production. This low-voltage (0.7–1.3 kV), but high-resolution (better than 5 nm) SEM has 512×512 pixels TV-like images and dedicated software to carry out the dimensional measurements. The images can be printed out on a video printer or saved on disk using a frame grabber. The image, which is present in the memory of the machine and used in the calculation, unfortunately is not accessible in its digital form.

Imaging Systems

The computer of the imaging system used on the CD SEM was a Hewlett-Packard Vectra XU 6/200 computer connected to the local, internal network and the Internet, outfitted with 48 MB RAM, 3 GB hard disk, and a 230 MB magneto-optical drive. The ability to save the images on this drive and the access to the Internet gave a very effective way for data transference. In this system, the nonstandard, almost TV frequency images were captured with a DT 3152 type, high-speed frame grabber card (Data Translation). This image acquisition card is very useful for the digitization of SEM images, since it is capable of accommodating various scan speeds and can capture an image series as well with up to 2048×2048 pixels resolution. This system also served as the basis for the facility of SEM Monitor that uses the frame grabber in real-

time mode. For evaluation of the images, the Isaac Image Analysis System (Postek and Vladár 1995) was also used in this study, which is based on a Macintosh PowerPC 8500/120 personal computer.

Sample

An appropriate sharpness analysis sample is very important to this work. The qualities of such a sample were discussed in Part I of this work (Postek and Vladár 1998). Essentially, the sample must have fine details and yield reasonably noise-free images with good contrast at least in the upper magnification range. Beyond the platinum-coated, gold-on-carbon sample, which is found so far to be the best for this method, a sample suitable for CD SEMs was identified. It is a silicon wafer with an etching artifact, called “grass.” The grass is a result of preferential masking during reactive ion etching, which produced fine, 5–15 nm diameter random structures (in the case of this sample). The grass sample is conductive, can be used at high or low accelerating voltage, and its tiny tower-like structure (Fig. 1) withstands the contamination caused by electron beam interactions. The staged-structure, etched photoresist sample (utilized for Fig. 2) is supplied by Hitachi on the sample holder of the CD SEM to help the operator set the focus and astigmatism. This sample has fine details at very high magnifications as well.

Software

A variety of image processing software was used throughout this study. For capturing images on the CD SEM, the UTHSCSA Image Tool (Image Tool) was used, which is a public domain image processing and analysis program.

*Certain commercial equipment is identified in this paper to describe the experimental procedure adequately. Such identification does not imply recommendation or endorsement by the National Institute of Standards and Technology, nor does it mean that the equipment identified is necessarily the best available for the purpose.

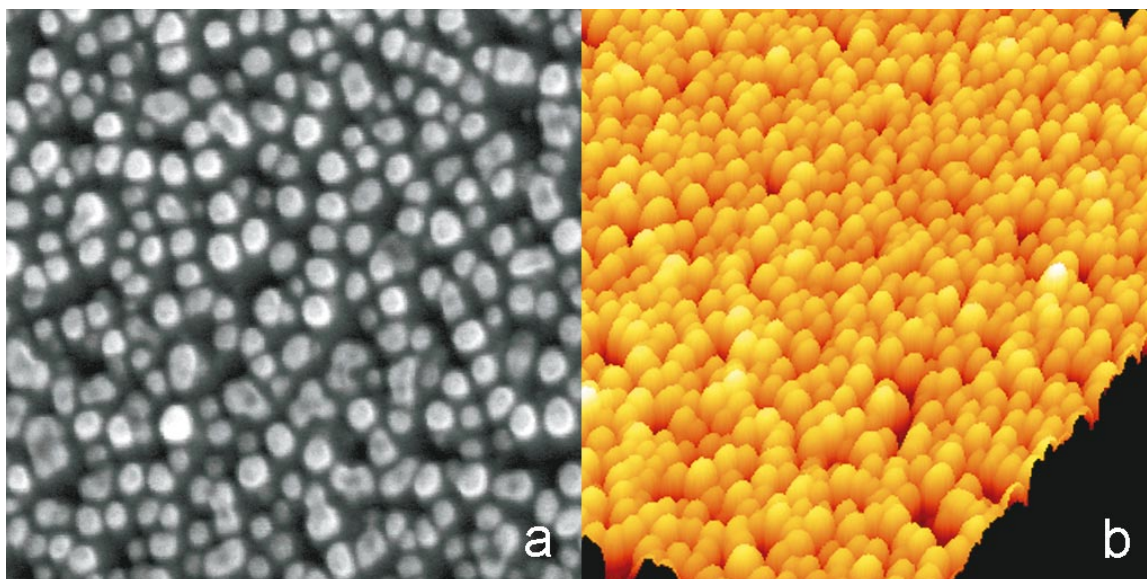


FIG. 1 Etched grass. (a) SEM image of an Si sample, “grass” that is a result of preferential masking during the reactive ion etching. (b) An atomic force microscope image that illustrates the three-dimensional structure of the grass sample. (Field width = 180 nm.)

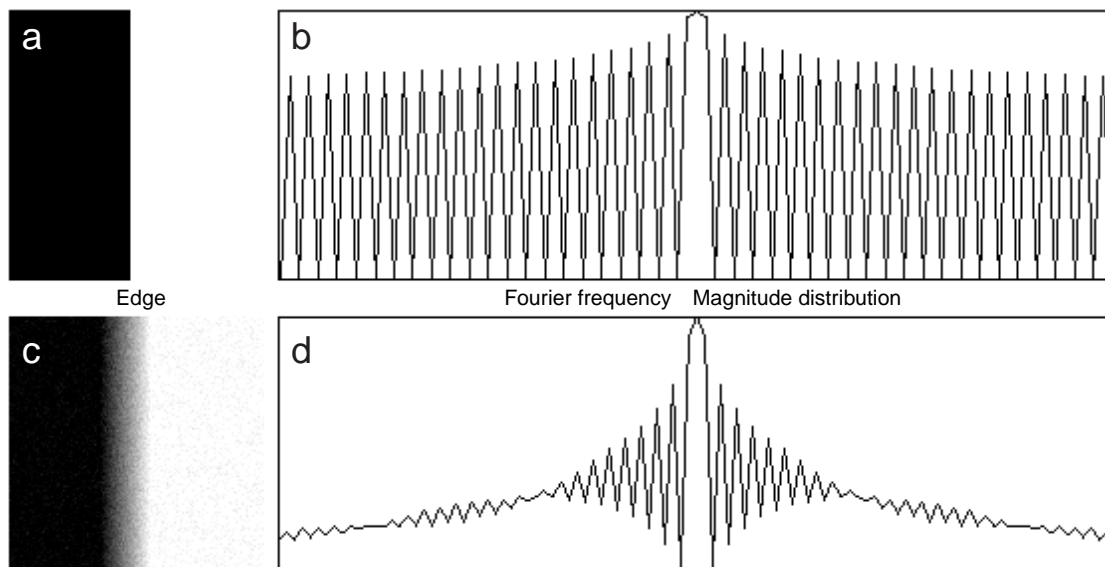


FIG. 2 Fast Fourier analysis. (a) Simulated image of a sharp line edge shown as a rapid transition from black to white (one-dimensional step function) and (b) the power spectrum. (c) Simulated image of a blurry edge and (d) its power spectrum.

Another public domain program, named NIH Image (Image) was also useful in this work. The fast Fourier calculations of isometric view images and the look-up table operations were made with this software. The real time calculations of the CD SEM images were carried out with SEM Monitor. This software on this system is able to provide data through fast Fourier calculations in every 0.6 s which is satisfactory for real time operation.

Fourier Transform

Very important image processing techniques are based on Fourier and inverse Fourier (and other frequency domain) transforms. Image compression or convolution and correlation methods are operating in the frequency domain, because these techniques are much faster than many similar operations in the original, spatial domain. The mathematical background of the Fourier transform is the theorem which states that it is possible to form any one-dimensional function $f(x)$ as a summation of series of sine and cosine terms of increasing frequency. The real variable x can represent time or distance in one dimension across an image.

The Fourier transform of a real $f(x)$ is generally a complex function: $F(k) = R(k) + jI(k)$ [where $R(k)$ and $I(k)$ are the real and the imaginary components]. The Fourier transform can be expressed in terms of an amplitude or magnitude by,

$$A(k) = \sqrt{R^2(k) + I^2(k)}$$

and a phase,

$$\Phi(k) = \tan^{-1} \left(\frac{I(k)}{R(k)} \right)$$

In this study, the calculations are limited to the use of the amplitude function. The variable k in the Fourier transform is called frequency variable. The Fourier transform can be extended to a function of two variables x and y . In practice, the various software packages use discrete Fourier transforms. The mathematical expressions for discrete functions are described in the literature (e.g., Gonzalez and Wintz 1977). The Fourier and inverse Fourier transforms are computed with powerful and very efficient algorithms such as the fast Fourier transform (FFT).

The magnitude distribution has a characteristic cone-like structure. In the origin, the zero frequency represents the overall brightness of the image, while the noise is visible around the outskirts of the cone. As the image gets sharper, that is, as the focus is improved, this cone widens and this change can be measured with a suitable method. The center part close to the origin carries the overall sample information and it is visible even on Fourier frequency magnitude distributions of quite blurry images.

Figure 2a shows an artificially generated image of a sharp edge. The transition is from black with values 0 on the left to white on the right with values of 255 (this is a one-dimensional step function). Figure 2b represents its power spectrum. Figure 2c is an artificially generated blurred edge with some noise added (to look similar to a real edge's image), and Figure 2d represents its power

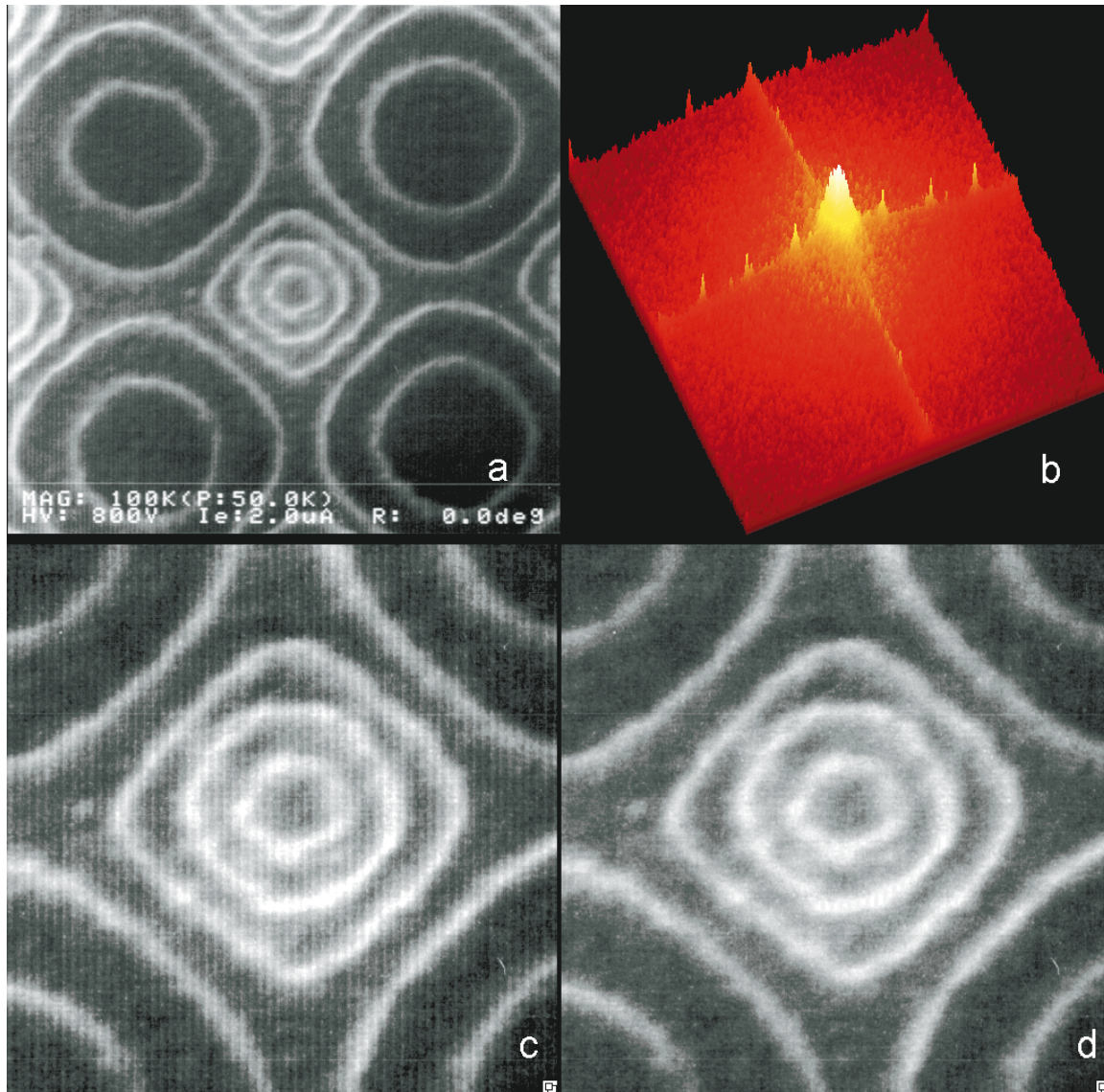


FIG. 3 Noise analysis. (a) Etched photoresist sample with some periodic noise induced in the image (field width = $1.15\ \mu\text{m}$). (b) An isometric view of the Fourier frequency magnitude distribution with the small peaks shown corresponding to the frequencies of the induced noise. (c and d) A digital magnification of the center part of (a) showing how this part looks before (c) and after (d) the offending noise was removed from the frequency distribution and an inverse Fourier transform was performed.

spectrum. The vertical axis on the graph is the frequency magnitude, while the parameter on the horizontal axis is frequency. Note that the distribution is symmetrical and the frequency amplitudes of the less sharp transition are rapidly diminished.

The SEM image contains information not just about the sample but also about the primary electron beam. In addition, the image is composed of all the parts contributing to the signal formation in the SEM (SE-1, SE-2, SE-3, and SE-4). Other than the useful signals, there are unwanted signals as well, for example, in the lower-frequency range the 60 or 50 Hz hum or vibration, shot and other noises in the high-frequency region may be included. The Fourier

method can be useful for analyzing certain noise components on SEM images. Figure 3a shows an image of the developed photoresist sample with some periodic noise. Figure 3b is an isometric view of the Fourier frequency magnitude distribution with small peaks corresponding to the frequencies of the noise. Figure 3c is a digital magnification of the center part of (a), and (d) shows how this part looks following inverse Fourier transform. Before the inverse transformation was applied, the small peaks related to the periodic noise were removed from the frequency magnitude distribution. Note that this operation very effectively removed the noise from the image while the fine details remained.

Sampling

A digital image is an array of two-dimensional samples of the continuous video signal. Since the Fourier calculation deals with the digitized form of the analog video signal, the sampling must fulfill the requirement of the Nyquist theorem in order to achieve correct results. This states that the sampling frequency must be at least twice as high as the highest frequency of the signal to be digitized, that is, sampled. For example, the 20 Hz–20 kHz audio signal on compact disks is recorded with 44.1 kHz sampling frequency. In the case of SEM images, it is easy to fulfill this requirement by setting suitable, high enough magnification.

Convolution

The image is the convolution of the describing geometry functions of the sample and primary electron beam. The convolution of two functions in the spatial domain is equal to the product of the Fourier transform of these two functions in the frequency domain. From an image, if the sample geometry is known, the geometric parameters of the primary electron beam are mathematically determinable. Even if the correct

description of the sample geometry is not known but invariable, from the calculations one can find out the best settings of the SEM to achieve the best possible resolution.

Results

Qualitative Evaluation of Sharpness

The sharpness analysis procedure begins with the calculation of the two-dimensional Fourier transform of an image using FFT techniques. Once the data array constituting the image is turned into Fourier magnitude and phase distribution, the evaluation of the sharpness can be done. For qualitative measurements, for example, to choose the best possible focus and astigmatism settings, simple color-coding of the magnitude distribution is adequate. This type of operation renders four colors to certain ranges of amplitude (density slicing). Figure 4 shows a series of SEM images (top), their Fourier magnitude distribution in logarithmic color-coded (center) and isometric views (bottom). The image of column (a) was taken by the operator as the best image, and as the four-level color-coding shows, the frequency magni-

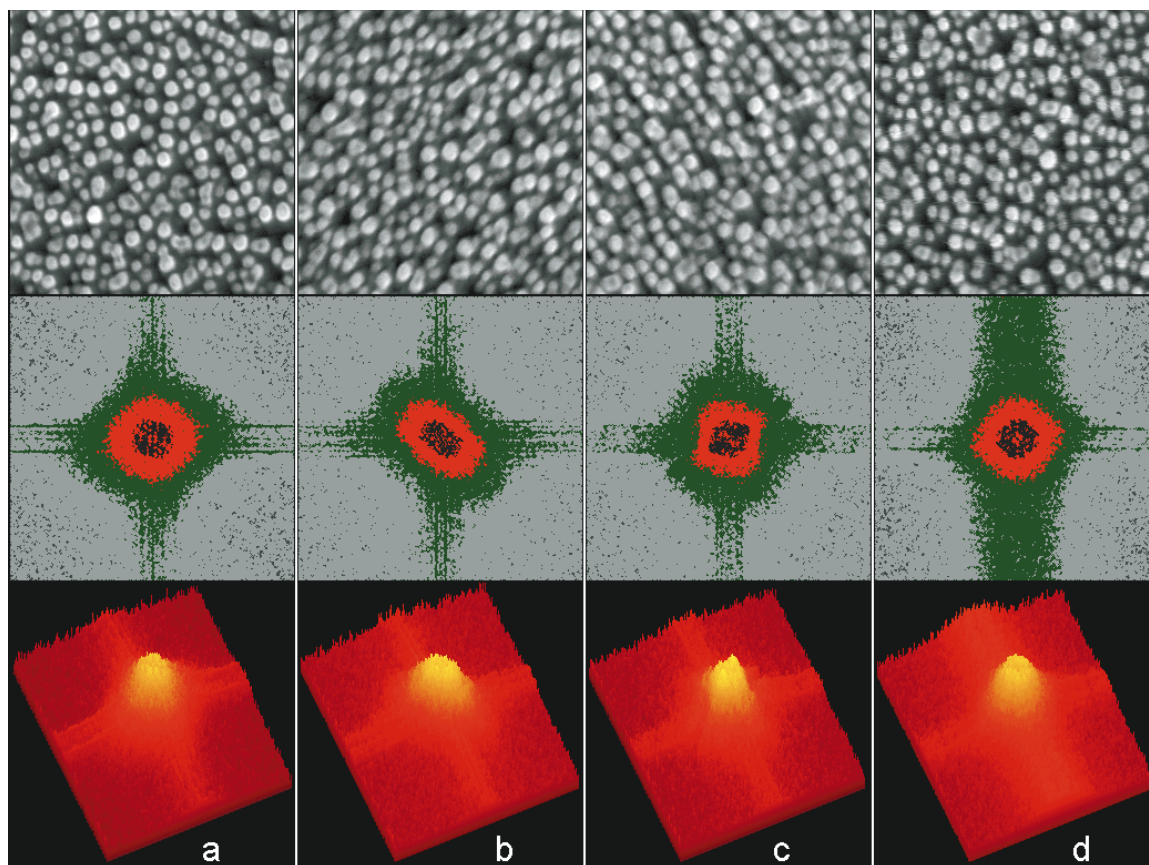


FIG. 4 Focus and astigmatism analysis. Columns (a) through (d) represent a series of images and their Fourier magnitude distribution in color-coded and isometric view. The images demonstrating various focus and astigmatism conditions (described in the text) were taken with a laboratory scanning electron microscope at 25 kV accelerating voltage at 100,000 \times magnification. (Field widths = 180 nm.)

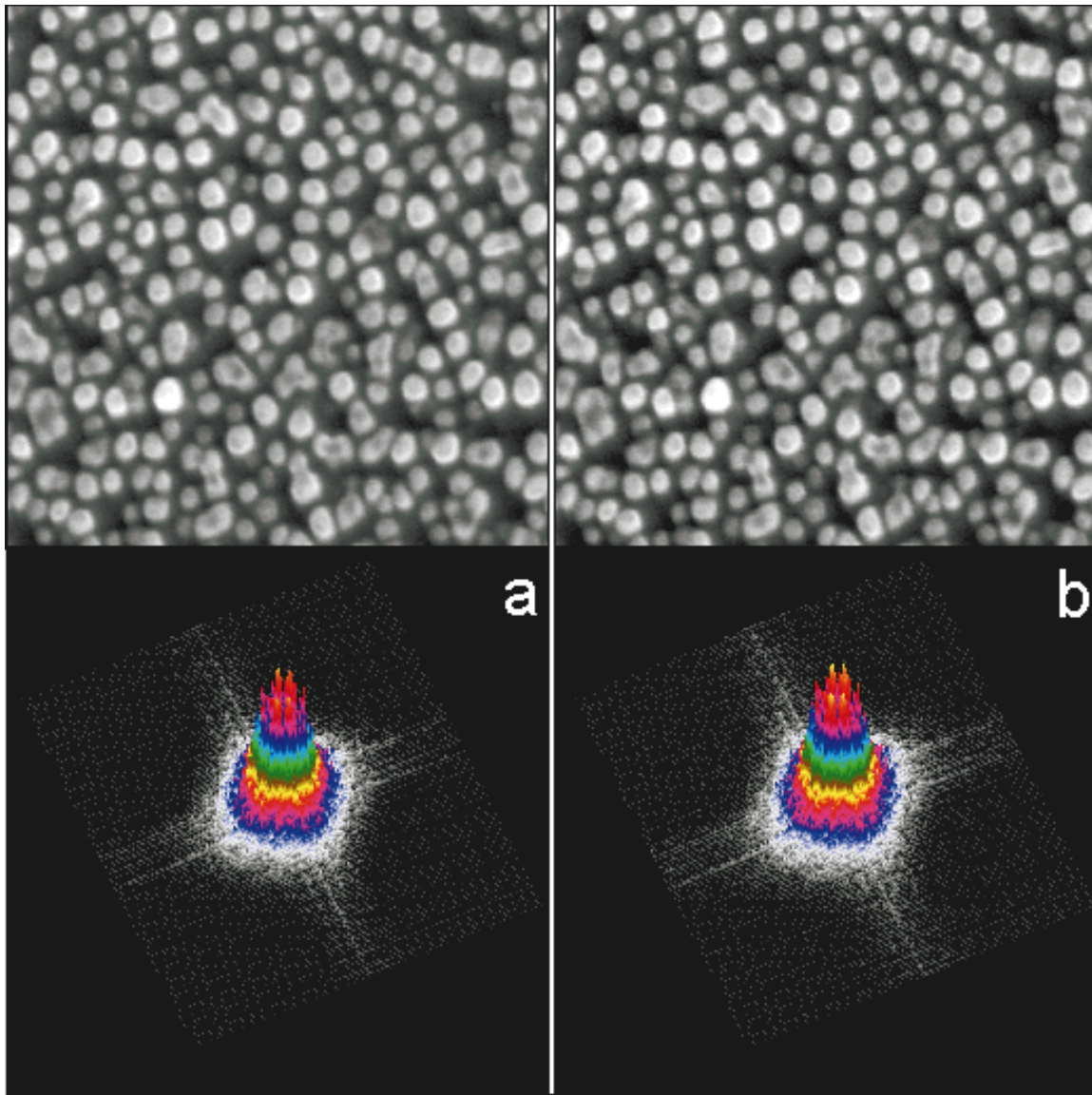


FIG. 5 Image of the “grass” sample. (a) is the original and (b) is the same image following image processing (sharpening and histogram stretching). The color-coded Fourier magnitude distributions are shown here in linear view. (Field widths = 180 nm.)

tude distribution is quite round at all levels. Image in column (b) was taken by changing the working distance. It is astigmatic and, as is well shown by the Fourier magnitude distribution, its shape is oval at all levels. If the electron optical column is well adjusted, the change of working distance results in focus change solely, that is, the frequency magnitude distribution gets smaller in diameter but it remains round. After proper setting, an even better, sharper image is possible. The image in column (c) appears to be somewhat fuzzy due to some noise, which makes the magnitude distribution distorted. This distortion is revealed on the density-sliced Fourier distribution by the nonsimilar shape of the slices, but can be seen better on the isometric view as wings on the characteristic cone. Image (d) is quite sharp but it has visible

noise caused by mechanical vibration of the sample stage. The isometric view shows an elevation caused by the high-frequency components of this noise. For all of these images the Nyquist theorem is fulfilled; the useful frequencies occupy only less than half of the Fourier frequency space, but this is not true for the noise of image (d), where the frequency components go beyond the boundaries.

Figure 5 shows an image pair. Image (a) on the left is the original, (b) is the same image after some processing (sharpening and histogram stretching). The Fourier magnitude distributions are shown here in linear view. To show the important part of the distributions, the center, the very high-amplitude part was removed. Although the images are clearly different, it is difficult to see this difference on the Fourier

magnitude distributions. Quantitative evaluation is needed.

Quantitative Evaluation of Sharpness

It is relatively easy to find quantitative procedures that yield numbers related to image sharpness. For certain samples it is enough to use simple image analysis functions, but to make the evaluation process robust and fast, special hardware and software are necessary. These techniques have been integrated into SEM Monitor.

SEM Monitor is designed to be a diagnostic aid for automated and semiautomatic SEM-based linewidth metrology. This program is also useful for monitoring the performance of laboratory instrumentation. It provides a quantitative framework for monitoring the SEM's sharpness, astigmatism, and image quality over time. SEM Monitor can also be used to aid in focusing the electron beam and correcting for astigmatism by providing feedback to the operator as he adjusts the instrument. Figure 6 shows the real-time window with the analysis of the above-mentioned photoresist sample using the CD metrology SEM. The trend chart in the lower right hand corner shows how the sharpness and astigmatism changed as the operator obtained a sharper image in three steps. The beam

shape monitor and the trend chart provide visual guide to adjusting the instrument. The screen refresh rate depends on settings, but the refresh rate can be as fast as 0.6 per s using a 200 MHz Pentium Pro system. Further improvements to throughput are being worked on.

SEM Monitor calculates the following values: angle and principal axes, eccentricity, and, of course, sharpness. The following section explains the meaning of these parameters and how they are derived.

Angle and Principal Axes

Let $P(k_x, k_y)$ denote the Fourier power ($A(k_x, k_y)^2$) for x and y directions. The moments are calculated similar to the moment of inertia tensor from mechanics, but instead of mass the Fourier power is used. The "Moment of Inertia" tensor I_{ij} can be written as:

$$I_{ij} = \frac{\iint P(k_x, k_y) W(k_x, k_y) k_i k_j d^2 k}{\iint P(k_x, k_y) W(k_x, k_y) d^2 k} \quad (1)$$

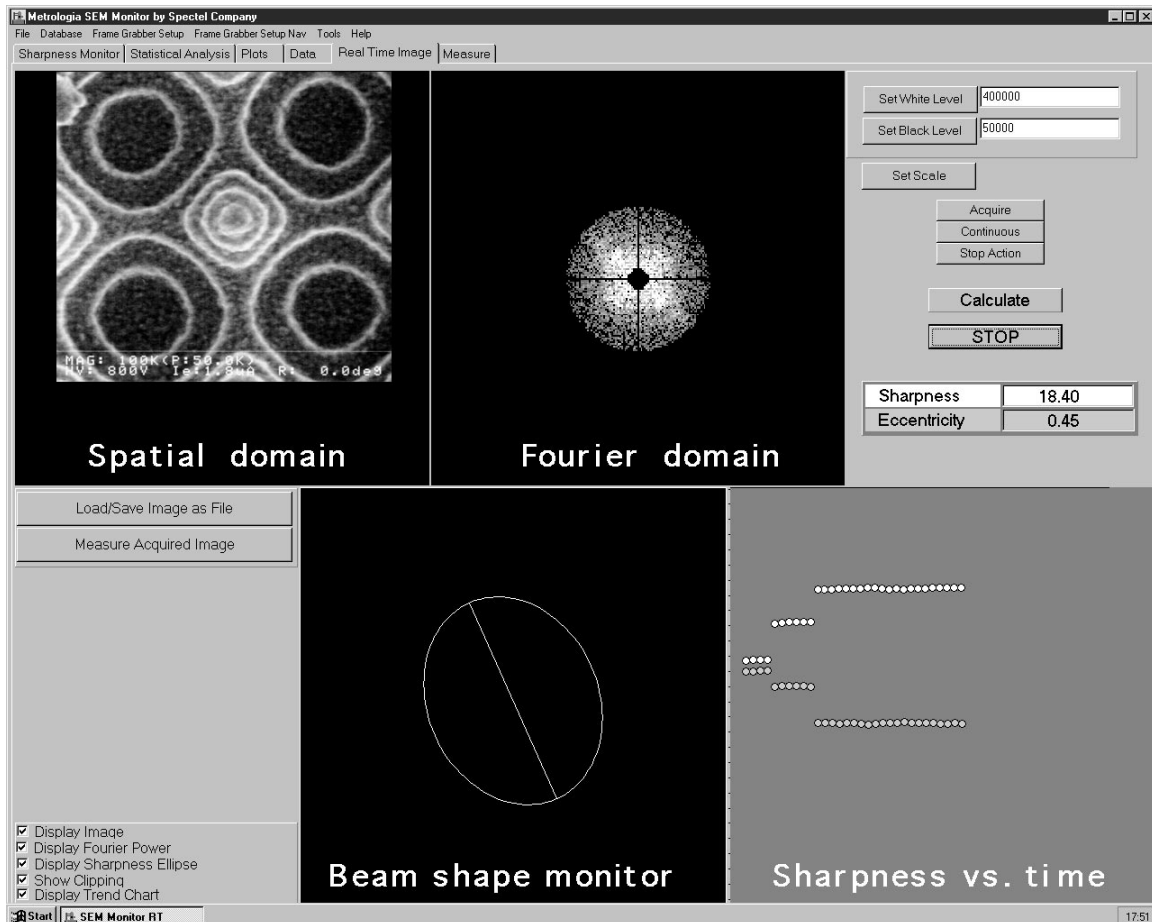


FIG. 6 SEM Monitor's Real-Time window with the analysis of the photoresist sample. (Field width = 1.15 μm .)

In this formula W is a weighting function whose purpose is to emphasize or de-emphasize different regions of k space. We would like our definition of sharpness to be insensitive to scaling of the signal which can occur if the gain of the SEM electronics drifts. To achieve this, the tensor in Eq. (1) is normalized by the total (weighted) Fourier power. The result has to be independent of a DC offset shift, that is, brightness change in the image, so values belonging to 0 on the x and y axes are excluded from the integration. In the discrete case the moment of inertia tensor becomes a two-dimensional sum.

The tensor I_{ij} can be diagonalized by rotating the coordinate axes, and the diagonalizing coordinate directions are called the principal axes and the diagonal values of the moment of inertia tensor are called the principal values. The diagonal elements of I are denoted by “Principal Axis 1” and “Principal Axis 2” in the output of SEM Monitor. The reported “sharpness” parameter is the smaller of the two principal values.

Eccentricity

Assuming that Principal Axis 1 (P_1) > Principal Axis 2 (P_2), then the “Eccentricity” is defined as:

$$\text{Eccentricity} = \sqrt{1 - \frac{P_2}{P_1}} \quad (2)$$

The angle reported is the angle between the original x axis and the direction of the Principal Axis 1. This can be thought of as the major axis of an ellipse. The ellipse in Fourier space is dual to the ellipse of, say, the beam profile in real space for an astigmatic image. In other words, if the beam were smaller in diameter in the x direction than in the y direction, this

would tend to produce a Fourier image that was narrower in y than x direction as shown in the beam shape monitor portion of Figure 6.

If the primary electron beam is scanning the sample with geometry distortions (barrel, pin-cushion or other) or non-square aspect ratio of the pixels, the Fourier calculations may not show zero eccentricity even with a perfectly round electron beam. Relative measurements can still be done or first a short calculation can be done to compensate for the distortions.

In SEM Monitor, the results are presented graphically as well as numerically. The graph displays an ellipse whose major and minor axes are proportional to Principal Axis 1 and Principal Axis 2, respectively. In moment of inertia terminology this is known as “Euler’s ellipse.”

The Weighting Function, W , includes a mask to eliminate certain regions from the integral in Eq. (1). Therefore, W is of the form:

$$W(k_x, k_y) = w(\vec{k}) \text{Mask}(k_x, k_y) \quad (3)$$

The Mask function takes on values 0 or 1. It is zero in those regions which are masked out. The mask is described in terms of a Maximum Radius, a Minimum Radius, and Zero Band. These are defined as follows:

Minimum Radius: The minimum radius is the interior portion of the FFT data which the sharpness algorithm can exclude from further analysis. This is a circle whose diameter is defined by the user. This permits the removal of the high peak in the center of the cone representing the brightness of the micrograph.

Maximum Radius: The maximum radius is the portion of the FFT data the sharpness algorithm excludes from further

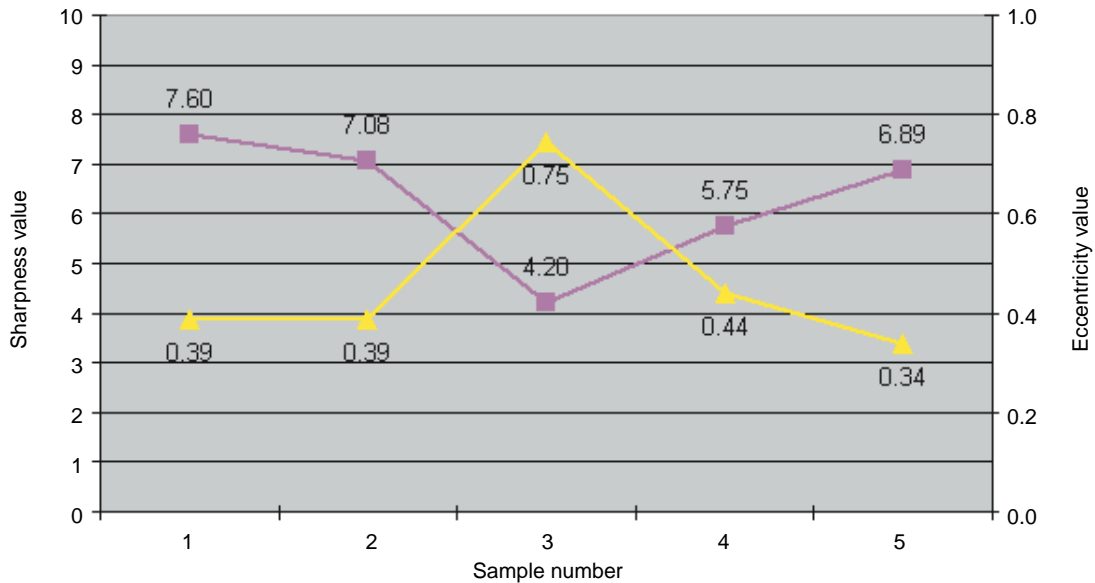
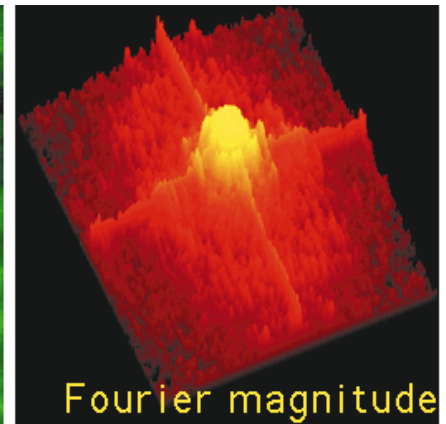
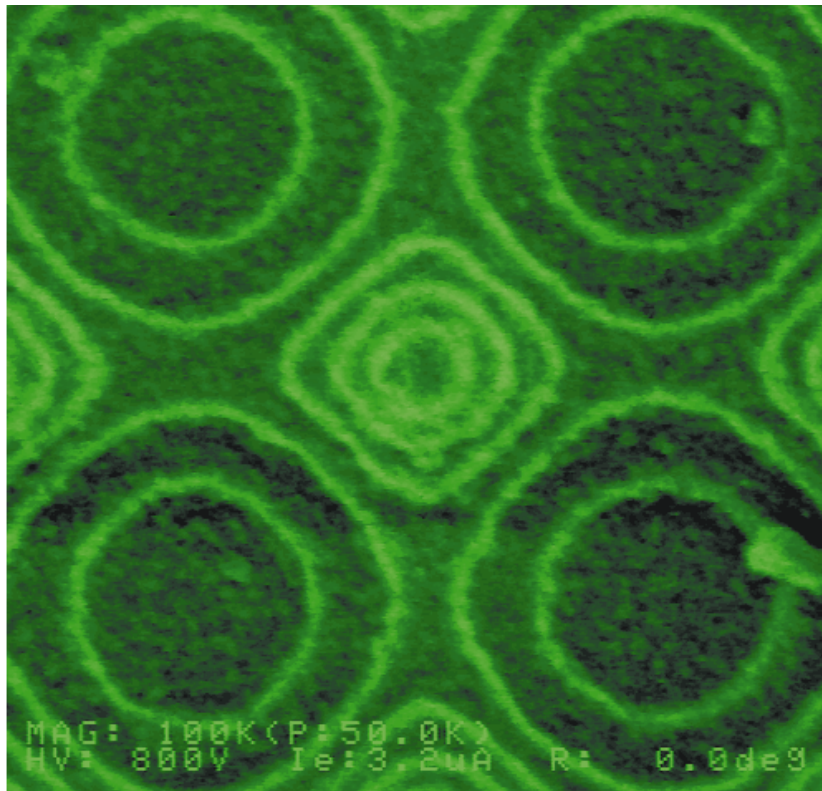


FIG. 7 Results of sharpness calculations of a series of images. Sample 1 is the processed image shown in Figure 5b, sample 2 is the image in Figure 5a or 4a, samples 3, 4, 5 are the images in Figure 4b, c, and d, respectively.

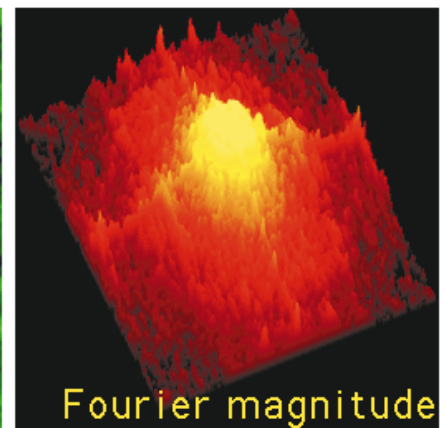
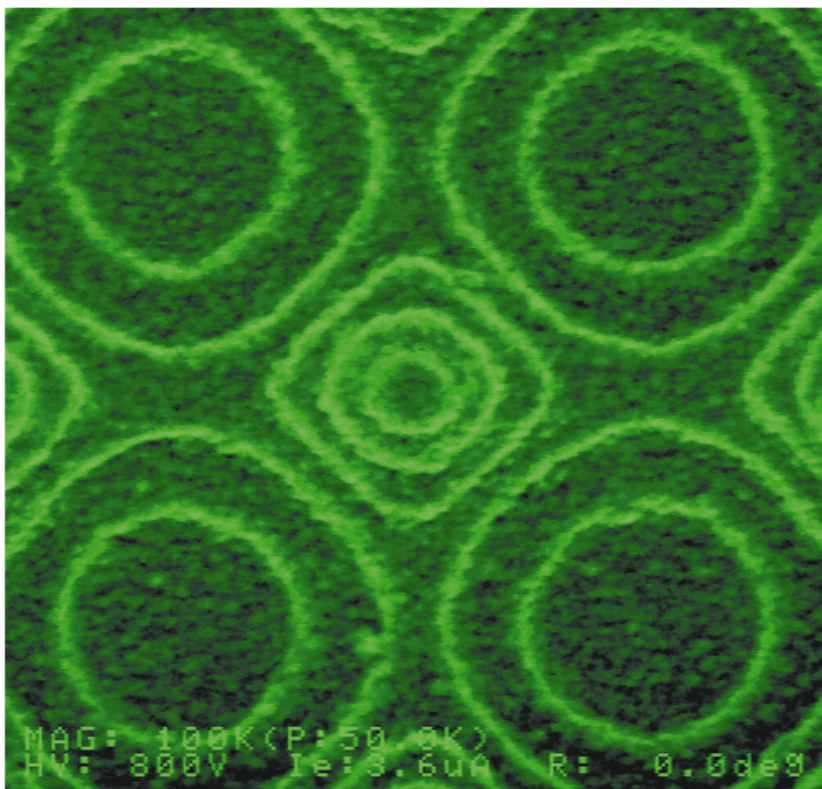


Line width:

242.5 nm

STD:

5.42 nm



Line width:

238.1 nm

STD:

4.37 nm

FIG. 8 Instrument performance and its effect on measurements. Shown is a summary of 25 linewidth measurements and their standard deviations for lines viewed in a production-line scanning electron microscope (SEM) measurement tool. The width measurements on the top were taken when the instrument was operating at a poorer performance level shown by the micrograph in the upper left and a more optimum performance level at the bottom after changing the objective lens aperture and proper adjustment of the electron optical column. The images clearly illustrate the difference in the performance of the SEM. (Field widths = 1.15 μm .)

analysis and which are outside a circle whose diameter is defined by the user. This parameter permits the restriction of the analysis to the frequencies of interest and excludes extraneous noise from the calculation.

Zero Band: The Zero Band value is the halfwidth of a band of elements about the k_x and k_y axes which is zeroed out before calculating the sharpness. The purpose of the Zero Band is to eliminate noise from consideration near to the k_x or k_y axis. Such noise can come from different sources: sample vibration and shift—line to line shift noise; or from a nonrepeating target so that the left edge and right edge or top and bottom are not the same. The discrete FFT treats the image as if it repeated itself in both the x and y directions periodically out to infinity; so, in a sense, the left edge of the picture and the right edge are adjacent. If the image data at these two edges are different, then the FFT treats this as a discontinuity in the x direction, and this appears as Fourier power spectrum all the way out along or near to the x axis. This noise is not exactly right on the x axis because, in general, it has some y variation to it. The same is true for the y direction. This noise can be reduced by choosing a target that looks like an island surrounded by a constant image intensity out to the border of the image. Then the image will have the right repetition and there will be no false Fourier frequency magnitude values. If one does not use such a target, one can choose the Zero Band to be large enough to reduce the importance of this noise in the sharpness calculation.

It is advantageous to impose threshold and saturation parameters on the Fourier power function before doing the moments calculation. The sharpness algorithm applies a threshold to all the data before doing its calculations. The threshold is expressed as a percent of the maximum value of the power spectrum. Data points that lie below the threshold value are set to zero. The sharpness algorithm applies a saturation level to all the data before doing the calculations. The saturation level is expressed as a percent of the maximum value of the power spectrum. Data points that lie above the saturation value are set to the saturation value; data points below the saturation value are not affected.

Sharpness

The results of the sharpness calculation are dependent on at least three parameters: the sample used, the values for all the settings, and the magnification of the instrument. In order to use the sharpness to compare different instruments, care must be taken to ensure that all these variables are the same: object (this means the same location on the object, too), instrument magnification, parameter settings (i.e., accelerating voltage, working distance, etc.). If all these conditions are fulfilled, then, in principle, the sharpness measure can be used to compare different instruments.

Figure 7 shows a graph with the results of sharpness calculations of a series of images. Sample 1 is the processed image shown on Figure 5b; Sample 2 is the image from Figure 5a or 4a; Samples 3, 4, and 5 are the images from Figure 4b, c, and

d, respectively. The sharpness values are different for the processed and unprocessed image (while the eccentricity stays the same).

Performance Monitoring

Scanning electron microscopes are being utilized extensively in the semiconductor production, and these instruments are approaching full automation. Once a human operator is no longer monitoring the instrument's performance and multiple instruments are used interchangeably, an objective diagnostic procedure must be implemented to ensure data and measurement fidelity. The correct setting of the sharpness and the knowledge of its value are very important for these production line instruments. Figure 8 shows a summary of 25 linewidth measurements and their standard deviation for photoresist lines viewed on an automated CD SEM tool. The measurement of the lines with this instrument resulted in an average of 242.5 nm for the width of the lines. The top left micrograph is an image of the photoresist test sample. Under these conditions, the instrument was functioning more poorly than evidenced by the lower left figure. The performance of the instrument was improved after changing the objective lens aperture and correctly adjusting the electron optical column. The same photoresist lines were measured again and their width was 238.1 nm on average, with a much smaller standard deviation. The greater than 4 nm difference in the measurement, resulting from the performance difference of the same instrument, is important to the production engineers, especially during the initial development phases of a new generation of integrated circuit manufacturing technology. With increasingly smaller linewidths on the horizon, the correct setting of the SEM becomes indispensable.

Conclusion

The technique described in this and the previous paper (Postek and Vladár 1998, Part I) can be used to check and optimize two basic parameters of the primary electron beam, the focus, and the astigmatism. Furthermore, this method makes it possible to check regularly the performance of the SEM in a quantitative, objective form. The short time required to use this method enables it to be performed before every critical measurement. To be able to get objective, quantitative data about the resolution performance of the SEM is important, especially where high-resolution imaging or accurate linewidth metrology is a concern. The Fourier method image analysis in the frequency domain summarizes all the transitions of the video signal constituting the whole image, not just one or some lines, in given directions. This improves the sensitivity (signal-to-noise ratio) and gives the focus and astigmatism information at once. The best solution would be if this and other image processing and analysis functions were incorporated as a built-in capability for all research and industrial SEMs.

Acknowledgments

The authors would like to thank Samuel N. Jones of the National Institute of Standards and Technology for his assistance in obtaining some of the SEM images used in this paper. They would also like to thank and acknowledge support for this work by the National Semiconductor Metrology Program (NSMP) and SEMATECH (Contract #96106772).

References

Data Translation, Inc. 100 Locke Drive, Marlboro, MA 01752-1192;
<http://www.datx.com/>
 Gonzalez RC, Wintz P: *Digital Image Processing*. Addison-Wesley Publishing Co., Inc. (1997) 41-45; ISBN 0-201-02597-3

Image Tool: Image Tool is available free on Internet at
<http://ddsdx.uthscsa.edu/dig/itdesc.html>

The authors of this software are C.D. Wilcox, S.B. Dove, W. D. McDavid and D. B. Greer. of the Department of Dental Diagnostic Science at The University of Texas Health Science Center, San Antonio, Texas, USA

Image NIH: Image is available free on Internet at
<http://rsb.info.nih.gov/nih-image/>

The author of this software is Wayne Rasband of the National Institutes of Health (NIH), NIMH Bethesda, MD 20892, USA

Postek MT, Vladár AE: Image sharpness measurement in scanning electron microscopy—Part I. *Scanning* 20, 1-9 (1998)

Postek MT, Vladár AE: SEM sharpness evaluation. *Proc MSA 1996* (Eds. Bailey GW, Corbett JM, Dimlich RVW, Michael JR, Zaluzec NJ). 142-143 (1996a)

Postek MT, Vladár AE: SEM sharpness evaluation using the sharpness criterion. *Proc SPIE* 2725, 504-514 (1996b)

Postek MT, Vladár AE: Digital imaging for scanning electron microscopy. *Scanning* 18, 1-7 (1995)